

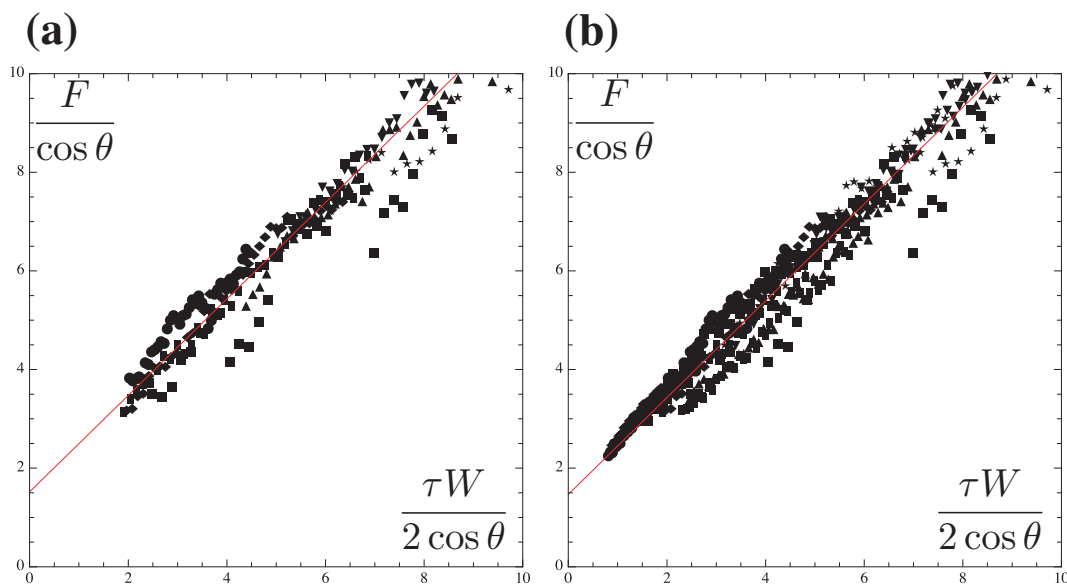
Supplementary Information for “Tearing as a Test for Mechanical Characterization of Thin Adhesive Films”

(E. Hamm, P. Reis, M. LeBlanc, B. Roman and E. Cerda)

Measurement of the fracture force

The intercepts in Fig. 3 show only an estimation of the fracture force since the straight lines intersect the y axis at $F = \gamma t \cos \theta$. Thus, the intercept in those figures also depends on the tear angle. To obtain a better estimation of the fracture force, we extract the adhesion from the slopes in Fig. 3 and plot the data using the modified equation (4)

$$\frac{F}{\cos \theta} = \frac{\tau W}{2 \cos \theta} + \gamma t \quad (\text{S1})$$



Supplementary Fig. 1: Measurement of the fracture force. a, Analysis of the data for M70 shown in Fig. 3b inset after forcing the slope to have an unit value. b, The same for all the data in Fig. 3b and Fig. 3b inset.

Supplementary Fig. 1a shows the data of Fig. 3b inset rearranged using equation (S1). As we can expect, the slope for the best fit is ≈ 1 , but the plot shows something more interesting. All

the runs have a similar intercept that we measured to be $\gamma t = 1.5 \pm 0.1$ N where the uncertainty indicates one standard deviation of the mean.

Likewise, we can combine all the data in Fig. 3b that was obtained for the same material M70 when adhered to a different substrate. Supplementary Fig. 1b shows that the intercept remains the same. In fact, we obtain a better fit $\gamma t = 1.47 \pm 0.04$ N since we have a larger number of data points. The same protocol was also used to obtain the fracture force for the materials M50 and M90.

Discrepancy from triangular shape near the tip

Equation (8) is no longer valid when the flap width is so small that adhesion energy is comparable to the fracture force. This happens when $\tau \frac{W}{2} \approx \gamma t \cos \theta$ in equation (7), or $L = \gamma t \cos \theta / (\tau \tan \theta) \sim 1$ mm for the experimental parameters used in Fig. 1a. This could explain the crossover observed in Fig. 1a for $L < 1$ mm to a different regime. In this second regime, both stretching and bending effects must be taken into account to obtain the elastic energy and predict the observed tear shape near the tip. Thus, equations (6) and (7) are not valid, even though equations (4) and (5) still apply to this more complex case.

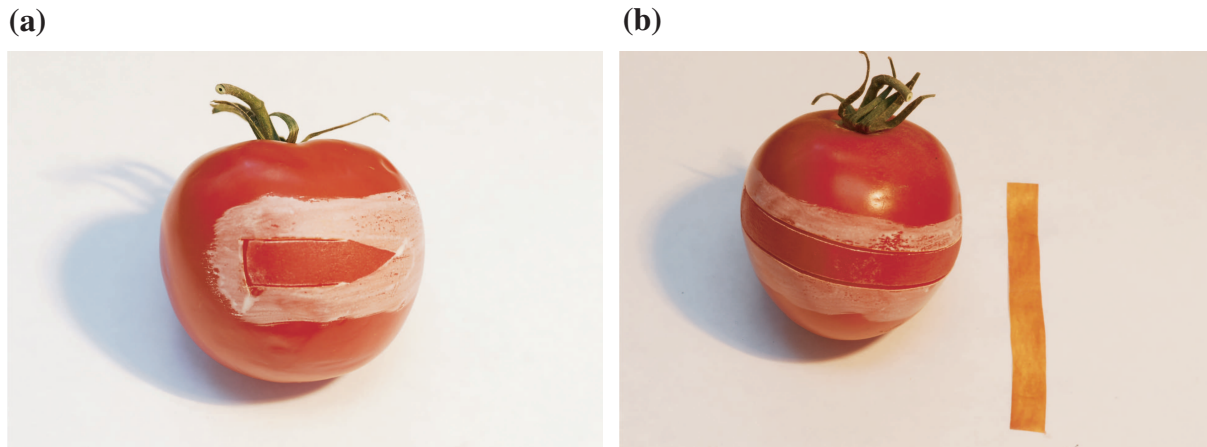
Equations (4) and (5) also yield a general framework to consider other physical situations when the films are not adhered to a substrate, but held on their boundaries and deform elastically. Again, when a flap is pulled to produce a tear, energy is localized in a narrow region connecting the flap with the film and becomes available for fracture. The specific geometry of the resulting fold gives a different elastic energy driving the fracture and lead to new tear shapes with no straight sides. Thus, under new conditions, different tear shapes can emerge that hide in their geometry the mechanism transforming elastic energy into surface energy of fracture and/or adhesion, and can potentially be used for mechanical characterization.

Skinning Tomatoes

The skin of fruits is a natural protective covering against physical and biological damage. This membrane is formed by nonliving cells that confer distinctive mechanical properties. Its higher stiffness, compared to the undersurface, makes it possible to peel-off the skin of the fruit and, in the process, we again obtain the scenario studied in this paper. The peeling leaves tears with triangular shapes that can be studied by the same formalism we developed for adhesive films.

Supplementary Fig. 2a shows the shape of a tear when a rectangular flap cut along the equator of a tomato fruit is pulled at a constant speed of $v \approx 5$ mm/s. The tear shape is approximately triangular and has an angle of $\theta \approx 20^\circ$. We can avoid this narrowing process by cutting two parallel lines with a surgical blade near the equator as Supplementary Fig. 2b shows. The tomato is now equivalent to a roll of tape. Long rectangular strips can be peeled off from the skin. It is important to note that the initial flap has a thickness of approximately 1 mm due

to the way we prepare it. However, after some distance of pulling, the skin thickness decreases and reaches a constant value of $t \approx 80\mu\text{m}$. Once the skin reaches this constant thickness, we deduced the effective adhesion from direct measurement of the pulling force. Our experiments gave $\tau \approx 80\text{ N/m}$ when the flap was pulled at a speed $v \approx 5\text{ mm/s}$.



Supplementary Fig. 2: Tears in tomato skin **a**, A 1 cm wide rectangular flap made along the equator of a tomato skin and pulled leaves triangular tears. Here the tomato was painted white before cutting the flap to better show the tear shape. **b**, The figure shows a tomato after a rectangular strip 1 cm wide was peeled from the equator. The narrowing process is avoided by cutting two parallel lines before pulling the flap. The strip of tomato skin is displayed beside it.

It is also easy to obtain the fracture force of the tomato skin by using the same rectangular strips detached from the fruit. We hung a strip vertically and cut a smaller flap of 5 mm that was pulled downwards by increasing weights until the tearing process started. This experiment gave a lower bound for the fracture force due to the deviation of the crack trajectories from their initial parallel directions (see equation (4)). It yielded a value $\gamma t \approx 8 \times 10^{-2}\text{ N}$. Thus, the work of fracture is $\gamma \approx 10^2\text{ N/m}$. This value can be compared with the experimental value reported in ref. 20 for tomato skin that is ten times smaller. This difference is not unusual in fracture mechanics when two tests use different modes of crack displacement. Reference 20 uses a tensile mode test while our method uses a tearing mode to fracture the surface.

It is much more difficult to measure bending stiffness. A strip of tomato skin has some natural curvature and must be hydrated while testing it. The setup described in the Methods section is difficult to implement in this case. On the other hand, our formula predicts a bending stiffness $B = (\eta\gamma t \sin\theta)^2/2\tau \approx 4 \times 10^{-6}\text{ J}$. Assuming that tomato skin is nearly isotropic²² and has a Poisson ratio $\nu = 1/2$, we conclude that the Young modulus is given by the formula $B = Et^3/12(1 - \nu^2)$ (see ref. 13). It gives $E \approx 70\text{ MPa}$. The reported values for the Young modulus of tomato skin ranging from 5 MPa to 50 MPa in ref. 20 are consistent with our estimation. However, the comparison should be taken with some caution since there are variations in the

mechanical properties between tomatoes of different species.

References

22. Karl J. Niklas, private communication.

Supplementary Movie

A long band of adhesive film 6 cm wide was attached to a glass and a rectangular flap of width 4 cm and length 5cm was cut and pulled to the right. Points T_1 and T_2 show the position of the cracks as fractures at each side of the flap propagate. The bright horizontal line shows the intersection of a laser sheet with the film. The deflection of this line, h , is proportional to the height that the flap is separated from the plane of the film. The last frame of the movie shows how the tear angle is obtained from the movie. Note that we do not measure the angle from the tear vertex since its sides are not straight (see Fig. 1a).